catalysts

MDPI

Article

Hydrocracking of Heavy Vacuum Gas Oil with Petroleum Wax

Olga Pleyer [1,*], Iva Kubičková [2], Aleš Vráblík [2], Daniel Maxa [1], Milan Pospíšil [1], Michal Zbuzek [2], Dominik Schlehöfer [2] and Petr Straka [1]

[1] Department of Petroleum Technology and Alternative Fuels, University of Chemistry and Technology, 160 00 Prague, Czech Republic; maxad@vscht.cz (D.M.); pospisim@vscht.cz (M.P.); strakap@vscht.cz (P.S.)
[2] ORLEN UniCRE a.s., Revoluční 1521/84, 400 01 Ústí nad Labem, Czech Republic; kubickoi@vscht.cz (I.K.); ales.vrablik@orlenunicre.cz (A.V.); michal.zbuzek@orlenunipetrol.cz (M.Z.); dominik.schlehofer@orlenunicre.cz (D.S.)
* Correspondence: smidkovo@vscht.cz; Tel.: +420-220-444-185

Abstract: Petroleum heavy vacuum gas oil (HVGO) containing 10 wt.% of petroleum wax was hydrocracked at 390–430 °C and under the pressure of 18 MPa over a Ni W/amorphous silica-alumina catalyst in a continuous-flow fixed-bed reactor. The hydrocracking of a reference feed (neat HVGO) was carried out under the same reaction conditions. The physico-chemical properties of primary products obtained via laboratory atmospheric-vacuum distillation (heavy naphtha, middle distillates and distillation residue) were evaluated. Most products prepared from the mixed feedstock had a similar or lower density and sulfur content than the products obtained from the hydrocracking of the neat HVGO. The heavy naphtha fractions obtained from mixed feedstock contained slightly more *n*-alkanes and *iso*-alkanes and less naphthenes and aromatics. Similarly, middle distillates obtained from the mixed feedstock contained slightly more *n*-alkanes and less aromatics and had cetane index higher by up to 2 units.

Keywords: heavy vacuum gas oil (HVGO); hydrocracking; petroleum wax; Fischer-Tropsch wax

Citation: Pleyer, O.; Kubičková, I.; Vráblík, A.; Maxa, D.; Pospíšil, M.; Zbuzek, M.; Schlehöfer, D.; Straka, P. Hydrocracking of Heavy Vacuum Gas Oil with Petroleum Wax. *Catalysts* **2022**, *12*, 384. https://doi.org/10.3390/catal12040384

Academic Editors: John Vakros, Evroula Hapeshi, Catia Cannilla and Giuseppe Bonura

Received: 23 February 2022
Accepted: 26 March 2022
Published: 30 March 2022

1. Introduction

Declining crude oil reserves together with the constantly increasing consumption of fossil fuels (diesel, gasoline, kerosene, etc.) and increasing emissions of greenhouse gases and other pollutants have prompted the increased global awareness of the new socio-economic and environmental challenge [1,2]. Consequently, research activities focused on the utilization of alternative and more preferably renewable energy resources are widely supported. At the current level of the state-of-the-art, liquid fuels are an indispensable energy carrier for the transportation sector due to the existing infrastructure (fuel distribution as well as engine technology) and their high energy density. The need for other carbon sources to produce liquid fuels can be satisfied only partially by renewable resources that can be converted directly into liquid transportation fuels, i.e., vegetable oils and fats (lipids) for biodiesel or hydrotreated vegetable oil (HVO) [3,4] and sugars for ethanol production [5]. Indirect routes of producing liquid transportation fuels from biomass offer a significantly larger potential particularly due to the abundance of lignocellulosic biomass and waste materials.

For the enhancement of liquid fuels production, several types of cracking processes (thermal cracking, catalytic cracking and hydrocracking) [6–8] are commonly applied. The hydrocracking of petroleum heavy vacuum gas oil (HVGO) is a commonly used process for the production of high-quality liquid fuels for vehicles and jet planes. The co-processing of heavy-vacuum gas oil with a high-molecular paraffinic feedstock can provide the additional intensification of the production of these high-quality liquid fuels. In consideration of the actual technological potential, the processing of the "synthetic" wax from Fischer-Tropsch synthesis (FTS) or the "natural" petroleum wax from the dewaxing process is possible [9].

FTS is one of the promising technologies of biomass conversion into the mixture of saturated hydrocarbons with a broad distillation range [10]. The achievable product distribution from FTS differs significantly from the current as well as expected fuel demands [11]. Moreover, due to the unsuitable physico-chemical properties of these fractions, such as the low octane number of the naphtha fraction and poor cold flow properties of the diesel fraction [12], they have to be further upgraded before being used as automotive fuel components. Beside the gaseous and liquid products of the FTS, a certain portion of the solid product, when boiling above 360 °C, is obtained. This product (called FTS wax) can be produced in high yields and then converted into the desired products by cracking technologies, such as fluid catalytic cracking (FCC) and hydrocracking [12–18]. The FTS wax is predominantly composed of *n*-alkanes (>95 wt.%) [5]. The concentrations of branched, unsaturated, and/or cyclic hydrocarbons (i.e., aromatics and naphthenes) in the FTS wax are very low; furthermore, it does not contain any sulfur or nitrogen-containing compounds. The congealing point of such paraffinic products typically exceeds 50 °C, so it is solid at an ambient temperature and requires further processing [19].

Petroleum waxes have similar characteristics to those of FTS waxes rather than crude oil distillation cuts [19,20]. Although these waxes are utilized in the production of cosmetics and packaging materials, there is a high potential hidden in their utilization for the production of automotive fuels because of their hydrocarbon-based nature and high energy content. FTS wax and petroleum wax can thus be considered suitable as feedstocks for cracking processes to produce high-quality diesel and gasoline-blending components.

The relatively high flexibility in terms of raw materials as well as in the distribution and quality of the products [21–23] is the main advantage of the hydrocracking processes. Consequently, hydrocracking processes have become the most common processes in new refineries. The general purpose of hydrocracking is threefold: (i) to crack the high-molecular-weight feedstock molecules to lower-molecular-weight products, e.g., in diesel fuel range, (ii) to remove hetero-atoms (S, N, O) and (iii) to reduce the aromatics content, especially the polynuclear aromatics content, to meet final product specifications.

In general, hydrocracking units are operated in the following range of operating conditions: 350–430 °C, 7–20 MPa, space velocity of 0.3–2.0 h^{-1} and hydrogen to feedstock ratio of 800–1800 Nm^3/m^3 [24]. Hydrocracking catalysts are typically bifunctional, with both metal (or metal sulfide) and acid sites. Their performance is determined by a balance between the metal (metal sulfide) sites and acid sites [25]. The metal (metal sulfide) sites are responsible for heteroatoms removal by hydrodesulfurization, hydrodeoxygenation, hydrodenitrification and for hydrogenation/dehydrogenation reactions. In terms of the hydrogenation/dehydrogenation function, hydrocracking catalysts can be divided into two classes, namely into sulfide-based metal catalysts (Ni–Mo, Ni–W or Co–Mo) and noble-metal-based catalysts (Pt, Pd). Since sulfur acts as a poison for Pt, Pd catalysts, they cannot be used for untreated petroleum feedstocks, but they are suitable for Fischer-Tropsch wax or other alternative feedstocks [26,27] as they are typically low in terms of heteroatoms content.

Halmenschlager et al. [28] carried out hydrocracking of HVGO containing 10 wt.% of FTS wax using sulfided $NiMo/SiO_2–Al_2O_3$ in a reaction temperature range of 330–410 °C and a pressure of 9.5 MPa and LHSV of 1.3 h^{-1}. Distillation curves, cold-flow properties, sulfur content, density and refractive index of the primary liquid products were determined. The presence of the FTS wax in the feedstock led to a decrease in the conversion. On the other hand, more intense hydrodesulfurization and denitrogenation was observed for the feedstock containing the FTS wax.

The objective of this work is to assess the influence of petroleum wax addition in conventional hydrocracking feedstock (heavy vacuum gas oil from crude oil distillation) on the overall conversion and the yields of the main hydrocracking products, i.e., naphtha, middle distillate (diesel) and hydrocracking residue, as well as on their composition and properties using a commercial hydrocracking catalyst.

2. Results and Discussion

The distillation curves of heavy vacuum gas oil (HVGO), petroleum wax (PW) and the mixed feedstock obtained via simulated distillation are presented in Figure 1. While the HVGO was entirely composed of components boiling above 400 °C, the PW contained approximately 40 wt.% of the fraction boiling below 400 °C. From the other point of view, even though the heaviest components of the PW boiled below 550 °C, the HVGO contained ca. 10 wt.% of the fraction boiling above 550 °C. As expected, the addition of the PW to the HVGO shifted the distillation curve of the mixed feedstock to lower values.

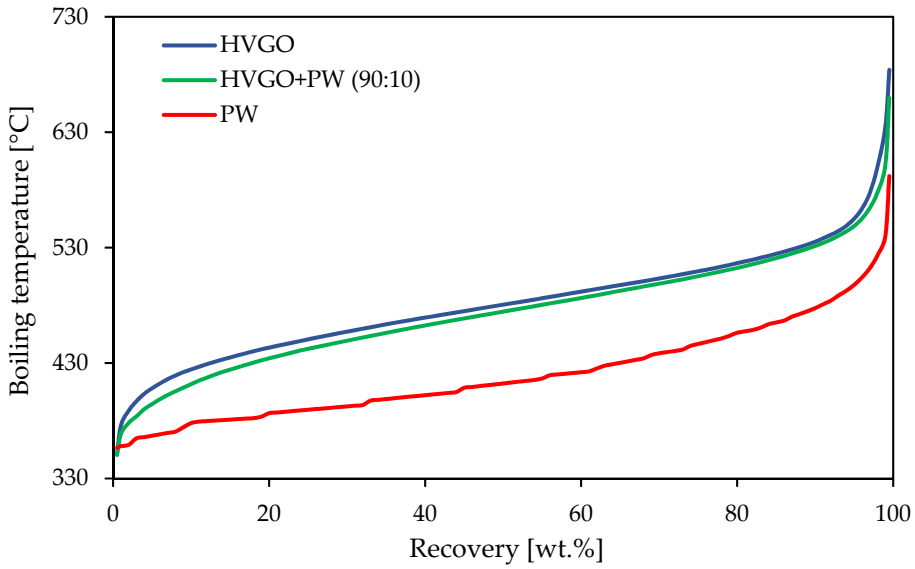

Figure 1. The distillation profiles of HVGO, PW and the mixed feedstock (simulated distillation).

Basic physiochemical properties of the HVGO, PW and the mixed feedstock used for the hydrocracking are presented in Table 1. The composition of the PW was determined via the GC-MS method showed that it was composed of ca. 88 wt.% of acyclic (predominantly unbranched) alkanes, 11 wt.% of alkylnaphthenes and less than 1 wt.% of other hydrocarbons. In comparison with the FTS waxes, the PW thus contained a higher proportion of the other hydrocarbons group than *n*-alkanes [2]. On the other hand, the content of aromatic components was very low, which supports the assumption of the PW and FTS wax similarity. The differences in the chemical composition of these two types of wax were thus considered as almost negligible and their manner during the hydrocracking should be very similar as well.

The density of the PW was significantly lower than the density of the HVGO which can be attributed to the lower distillation profile and the absence of aromatic structures in PW. On the other hand, its pour point was higher in comparison with HVGO. It can be associated with the chemical nature of the PW composed predominantly of saturated straight chain paraffins. The PW was sulfur and nitrogen free, which affected its overall elemental composition, so the dominant elements were carbon and hydrogen only. On the other hand, significant proportions of sulfur and nitrogen were detected in the HVGO and thus in the mixture feedstock as well.

The primary liquid products of the hydrocracking were characterized by their density at 25 °C and refractive index at 50 °C to operatively monitor the composition changes during the hydrocracking. The representative values of these parameters are given in Table 2 together with liquid feedstock conversion, liquid products yield and elemental composition.

Table 1. Basic physico-chemical properties of raw materials used in hydrocracking experiments.

Parameter (Unit)	HVGO	PW	HVGO + PW (90:10)
Density at 25 °C (kg·m^{-3})	927.3	845.1	919.1
Pour point (°C)	27	58	36
Refractive index at 50 °C	1.500	1.440	1.494
Elemental composition (wt.%)			
Carbon	84.60	86.15	84.77
Hydrogen	13.10	13.78	13.16
Sulfur	2.02	<0.001	1.82
Nitrogen	0.28	<0.001	0.25
Distillation [a]			
10 wt.% recovered at (°C)	425	378	412
50 wt.% recovered at (°C)	481	412	475
90 wt.% recovered at (°C)	535	478	532

[a] data obtained from the simulated distillation.

Table 2. Hydrocracking summary and basic properties of primary liquid products.

Parameter (Unit)	390 °C		410 °C		430 °C	
	HVGO	HVGO + PW	HVGO	HVGO + PW	HVGO	HVGO + PW
Yield of liquid (wt.%)	92.2	92.1	83.7	84.6	72.2	73.4
Conversion, 360 °C (wt.%)	29.8	28.2	62.0	60.9	91.4	86.6
Density at 25 °C (kg.m^{-3})	853.3	845.9	828.8	820.0	809.2	804.5
Refractive index at 50 °C	1.4709	1.4673	1.4578	1.4532	1.4478	1.4459
Elemental Composition						
Carbon (wt.%)	85.67	85.40	85.23	85.56	85.31	84.99
Hydrogen (wt.%)	14.21	14.50	14.73	14.41	14.65	14.97
Sulfur (mg·kg^{-1})	994	794	359	248	298	307
Nitrogen (mg·kg^{-1})	227	179	87	51	74	75
Distillation [a]						
10 wt.% recovered at (°C)	280	287	208	206	173	178
50 wt.% recovered at (°C)	441	436	379	379	302	315
90 wt.% recovered at (°C)	511	512	495	493	466	468

[a] data obtained from simulated distillation.

The yield of the primary liquid products decreased with an increasing reaction temperature. The influence of the PW addition to the feedstock was less significant, especially at 390 °C where the difference between products from both feedstocks was almost negligible. The application of the higher reaction temperatures caused a moderate increase in the liquid product yield from the feedstock containing the PW. The increasing reaction temperature was followed by the increasing conversion of the feedstock to the products with the required boiling range, i.e., below 360 °C. The addition of the PW to the feedstock led to a mild conversion reduction. Although it was possible to observe a slight density reduction caused by the addition of the PW to the feedstock, the differences between the density of the primary products decreased strongly with the increasing reaction temperature caused by the increasing conversion.

The decrease in the refractive index (RI) of primary liquid products with an increasing reaction temperature was evident. The decreasing RI was caused by the decreasing content of heterocompounds and aromatics and cracking of long-chain paraffins into shorter ones. For example, the refractive indexes of *n*-nonane, *n*-decane and *n*-dodecane at temperature 35 °C are 1.3989, 1.4062 and 1.4154, respectively [29]. The refractive index can therefore be used as a parameter for the fast and operative monitoring of the hydrocracking process.

As expected, the more severe reaction conditions lead to deeper desulfurization and denitrogenation (Table 2). This observation is in accordance with the results of Halmenschlager et al. [28] who hydrocracked the mixture of HVGO and petroleum wax at a pressure of 9.5 MPa and the temperature range of 330–410 °C. The primary products obtained from the feedstock containing PW at the reaction temperatures of 390 and 410 °C had a lower sulfur and nitrogen content than similar products obtained from the neat HVGO. On the other hand, the content of sulfur and nitrogen in products obtained at a temperature of 430 °C was almost the same. This is probably due to the reaction of hydrogen sulfide and ammonia with alkenes formed as intermediates of hydrocracking of wax at a higher reaction temperature (430 °C) into aliphatic sulfur and nitrogen compounds (e.g., mercaptanes, sulfides, amines). For example, the direct hydrosulfurization and hydroamination of ethylene by hydrogen sulfide and ammonia on zeolites was described by Kalló et al. [30] and Deeba et al., respectively [31]. Nevertheless, in the industrial process, these sulfur and nitrogen compounds are easily eliminated by the hydrorefining catalyst at the end of the catalyst bed.

The distillation profiles of the primary hydrocracking products were more affected by the reaction temperature than by the feedstock composition (Table 3). As expected, the increasing reaction temperature shifted the distillation curves of the primary products downward to the lower boiling points and increased the yield of light fractions. On the other hand, differences between the distillation profiles of two products obtained at the same reaction temperature from various feedstocks were negligible.

Table 3. Physico-chemical properties of heavy naphtha fractions obtained by hydrocracking of HVGO and HVGO containing 10 wt.% of petroleum wax (HVGO + PW) at various temperatures.

Parameter (Unit)	410 °C		430 °C	
	HVGO	HVGO + PW	HVGO	HVGO + PW
Density at 15 °C ($kg \cdot m^{-3}$)	791.3	790.1	781.0	779.2
Sulfur ($mg \cdot kg^{-1}$)	14	13	17	17
Nitrogen ($mg \cdot kg^{-1}$)	13	11	11	14
Water ($mg \cdot kg^{-1}$)	36	47	35	32
Distillation [a]				
10 wt.% recovered at (°C)	140	141	139	138
50 wt.% recovered at (°C)	176	174	169	169
90 wt.% recovered at (°C)	197	196	192	193

[a] data obtained from simulated distillation.

The data presented in Figure 2 show that the yields of the light fractions (gases + light naphtha) and distillation fractions (heavy naphtha and middle distillates) increased with an increasing reaction temperature of hydrocracking. As the rate of cracking was rather low at the reaction temperature of 390 °C, considerable amounts of heavy naphtha were obtained only by hydrocracking at 410 and 430 °C. The products obtained from the mixed feedstock yielded slightly less than a middle distillate and slightly more distillation residue then the products obtained from the neat HVGO.

The heavy naphtha fractions obtained from hydrocracking at 430 °C had slightly lower distillation curves than the heavy naphthas obtained from hydrocracking at 410 °C. There were no significant differences between heavy naphthas obtained from different raw materials. Some other physico-chemical properties of the heavy naphthas are shown in Table 3. A high reaction temperature and the presence of the petroleum wax in the feedstock reduced the density of the obtained heavy naphthas, but the influence of the reaction temperature was much greater. The contents of sulfur and nitrogen were comparable for all samples with regard to their relatively low values. On the other hand, the slightly higher content of sulfur and nitrogen in products obtained at a temperature of 430 °C was probably caused by the presence of aliphatic sulfur and nitrogen compounds formed during the

hydrocracking. The reaction temperature also influenced the group-type composition of the heavy naphthas. The greatest effect was observed in the content of cycloalkanes (Figure 3), which represented the major group of all heavy naphthas. The content of cycloalkanes decreased by more than 4 wt.% when the reaction temperature was increased from 410 to 430 °C. The intensive opening of the naphthenic ring and subsequent formation of *n*-alkanes or *iso*-alkanes was, therefore, not observed. The opening of the naphthenic ring during hydrotreating requires strong hydrogenolytic functionality provided by noble metals [32]. The differences in cycloalkanes content between the naphthas obtained from the neat HVGO and mixed raw material were negligible. The content of aromatic hydrocarbons also slightly decreased with an increase in the reaction temperature. The naphthas obtained from raw material containing PW had a lower content of aromatics than the naphthas originating from neat HVGO. This could be attributed to the absence of aromatic hydrocarbons in the petroleum wax. On the other hand, the content of *n*-alkanes and *iso*-alkanes in products was higher at a higher reaction temperature, which is a consequence of the more extensive cracking and cleaving of aliphatic side-chains from alkyl-cycloalkanes and alkyl-aromatics. The addition of the PW into the feedstock caused a moderate increase in the content of *n*-alkanes and *iso*-alkanes of approx. 1 wt.%.

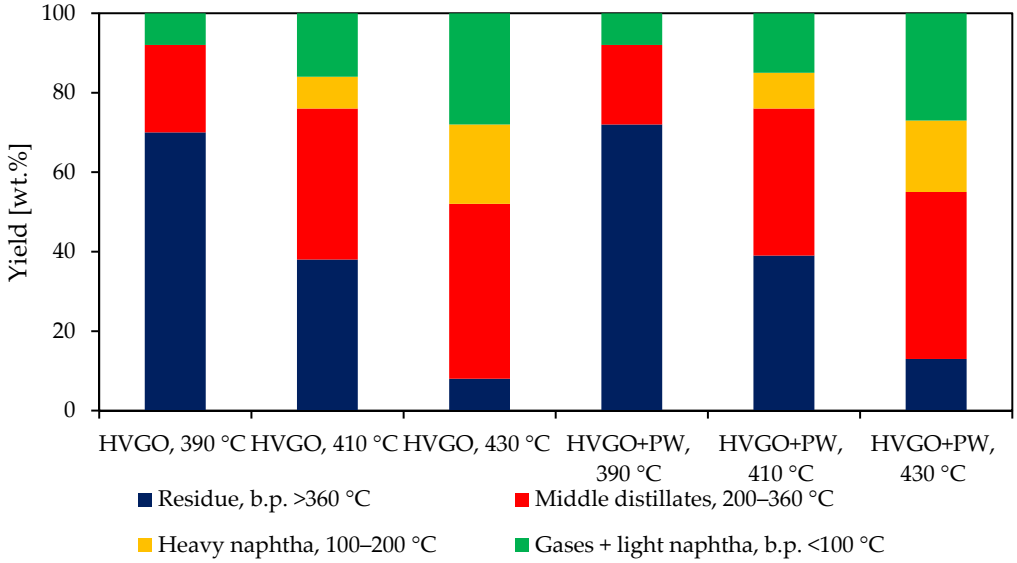

Figure 2. Fraction composition of the primary products obtained by hydrocracking of HVGO and HVGO + PW at various temperatures.

All middle distillates obtained from primary hydrocracking products had a similar distillation profile and their composition corresponded to that of diesel fuel. Table 4 shows physico-chemical properties of the analyzed middle distillates. Both products obtained from hydrocracking at 390 °C had the same density. The density of the middle distillates decreased with an increasing reaction temperature. Furthermore, density was influenced by the type of the feedstock to a greater extent than kinematic viscosity. The products obtained from the feedstock containing the PW had a lower density than those originating from the neat HVGO. The sulfur and nitrogen content in middle distillates showed a similar trend to primary liquid products. The content of sulfur and nitrogen increased slightly at the highest tested reaction temperature of 430 °C compared to the temperature of 410 °C. This is probably due to the presence of aliphatic sulfur and nitrogen compounds formed during the hydrocracking which can be easily hydrotreated on the hydrotreating catalyst placed at the end of the hydrocracking unit [5,6].

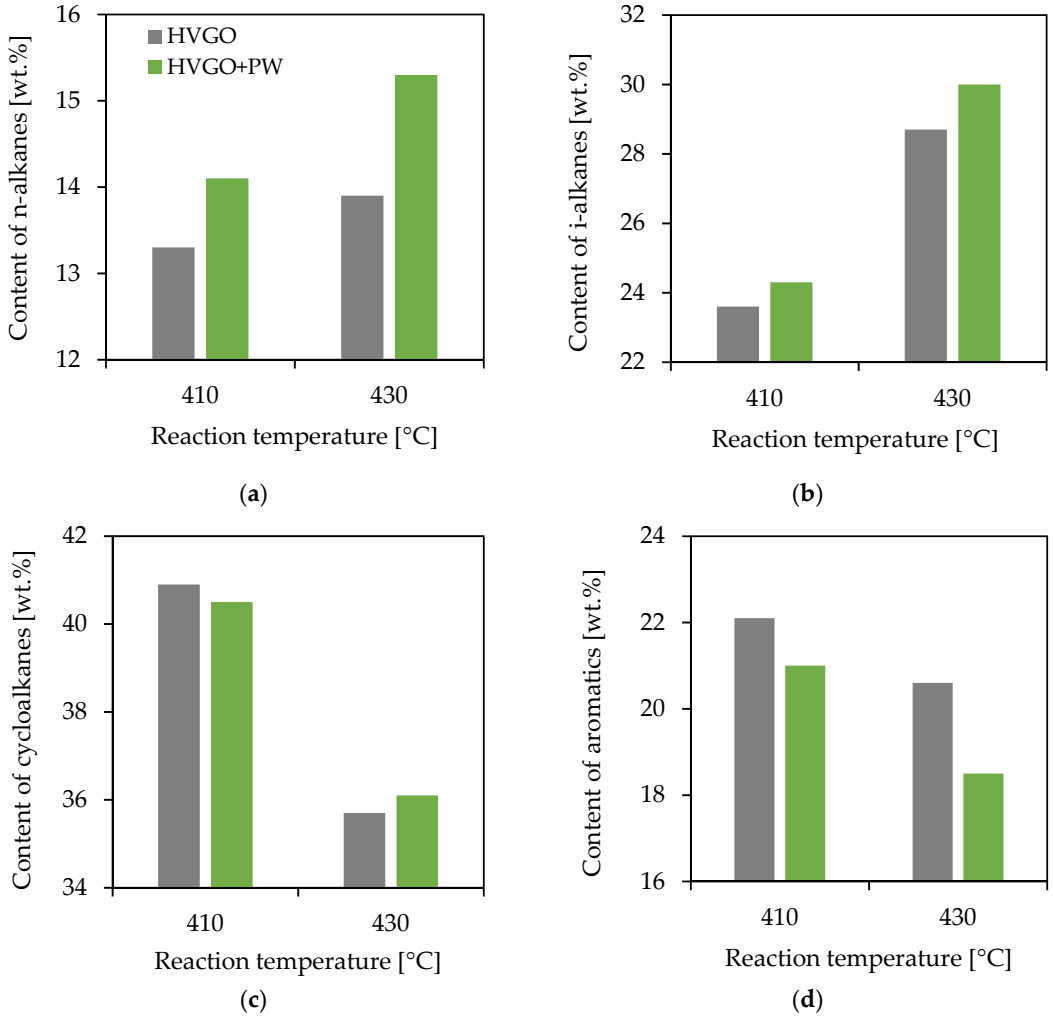

Figure 3. Group-type composition (*n*-alkanes (**a**), i-alkanes (**b**), cycloalkanes (**c**), aromatics (**d**)) of heavy naphthas obtained by hydrocracking of HVGO and HVGO containing 10 wt.% of petroleum wax (HVGO + PW) at various temperatures.

Table 4. Physico-chemical properties of middle distillates obtained by hydrocracking of HVGO and HGVO containing 10 wt.% of petroleum wax (HVGO + PW) at various temperatures.

Parameter (Unit)	390 °C		410 °C		430 °C	
	HVGO	HVGO + PW	HVGO	HVGO + PW	HVGO	HVGO + PW
Density at 15 °C ($kg \cdot m^{-3}$)	846.3	846.4	835.3	830.5	829.9	826.5
Viscosity at 40 °C ($mm^2 \cdot s^{-1}$)	3.08	3.16	3.16	3.00	2.73	2.77
Distillation [a]						
at 250 °C recovered (vol.%)	36	35	32	35	42	40
at 350 °C recovered (vol.%)	>95	>95	>95	>95	>95	>95
95 vol.% recovered at (°C)	311	315	316	309	310	311
Cetane index	47.5	48.1	53.8	55.0	53.3	55.3
Flash point (°C)	- [b]	- [b]	95	94	92	94
Sulfur ($mg \cdot kg^{-1}$)	140	120	52	32	63	72
Nitrogen ($mg \cdot kg^{-1}$)	48	40	14	9	15	18
Water ($mg \cdot kg^{-1}$)	20	21	41	52	21	30
Cloud point (°C)	−29	−29	−31	−28	−30	−28

[a] values equivalent to atmospheric distillation calculated using API correlation according to ASTM D2887 standard test method; [b] not measured due to a small amount of the sample.

The increase in the reaction temperature from 390 to 410 °C favorably influenced the cetane index (CI), but further increasing the reaction temperature to 430 °C did not lead to additional improvement in this parameter. All middle distillates obtained from the feedstock containing PW had a higher cetane index than those obtained from the neat HVGO (Table 4). Low temperature properties of middle distillates were excellent—the cloud point of all tested samples was lower than −25 °C (Table 4). Small differences not exceeding 3 °C are not significant.

The middle distillates contained approximately 5 to 8 wt.% of *n*-alkanes (Figure 4). Their content increased with an increase in the reaction temperature of hydrocracking. All distillates obtained from the feedstock containing the PW had a higher content of *n*-alkanes than those obtained from pure HVGO, the difference slightly increased with an increasing reaction temperature.

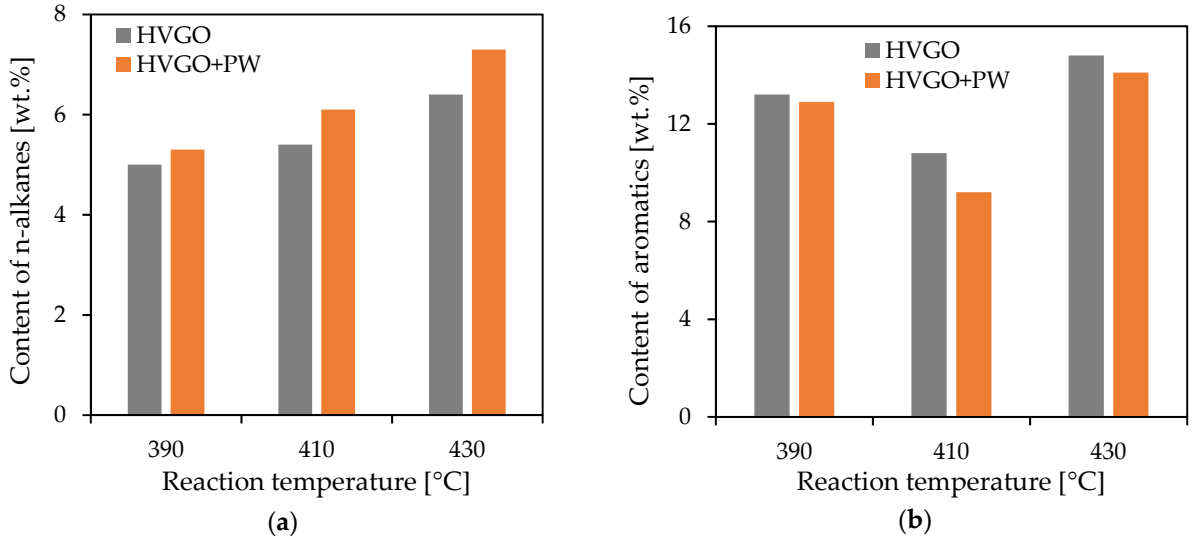

Figure 4. Group-type composition (*n*-alkanes (**a**) and aromatics (**b**)) of middle distillates obtained by hydrocracking of HVGO and HVGO containing 10 wt.% of petroleum wax (HVGO + PW) at various temperatures.

Correspondingly, all middle distillates obtained from the mixed feedstock contained a lower content of aromatic hydrocarbons than those originating from the neat petroleum raw material (HVGO). The dependence of the content of aromatics on the reaction temperature showed a minimum at 410 °C. This could be explained by the influence of temperature on reaction equilibrium. The formation of aromatic hydrocarbons is preferred at high reaction temperatures, even though the reaction mixture contains excess hydrogen, thereby promoting de-aromatization at mild temperatures and sufficient residence times. This hypothesis was confirmed by calculations of the theoretical composition of an equilibrium reaction mixture resulting from the hydrogenation of naphthalene with hydrogen (at 1000 L/L hydrogen/feed volume ratio and 18 MPa). Equilibrium conditions were considered such that the minimum Gibbs energy was attained. Figure 5 shows the effect of temperature on the equilibrium composition of the reaction mixture with an apparent increase in the naphthalene concentration at elevated temperatures. It can be concluded that the optimum reaction temperature is a compromise between the reaction kinetics of hydrogenation reactions and the equilibrium composition of a reaction mixture.

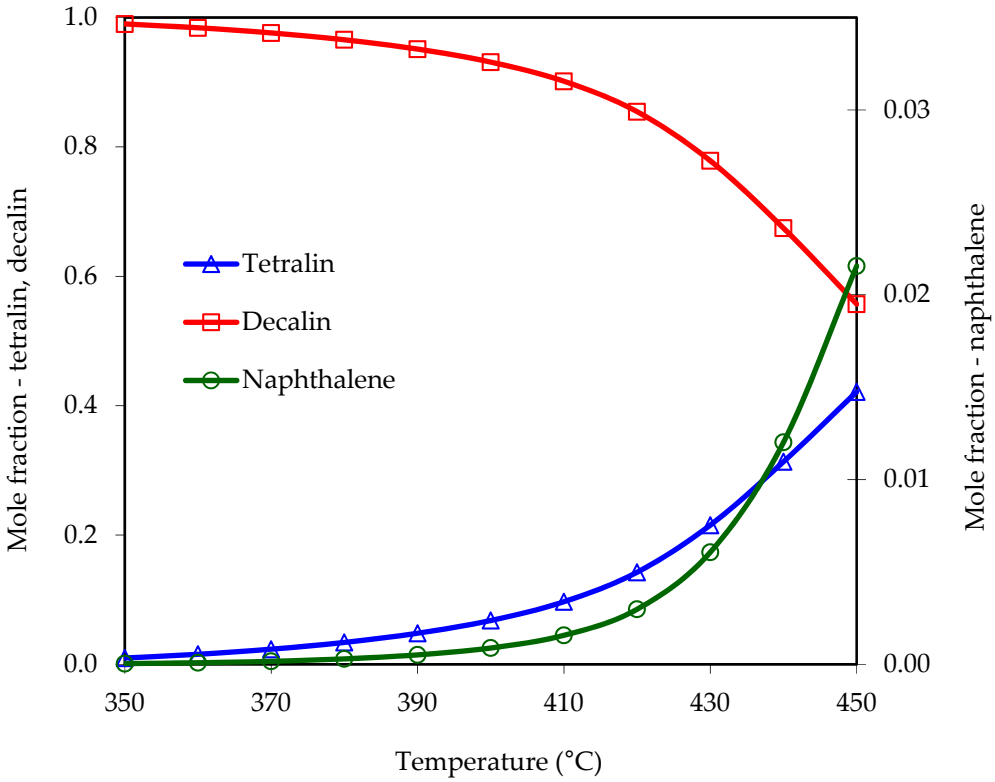

Figure 5. Equilibrium composition of a reaction mixture resulting upon hydrogenation of naphthalene (H_2/feed ratio of 1000 L/L, 18 MPa).

Although the content of other hydrocarbon groups was not determined directly, it can be expected that a major part of the middle distillates was composed of *iso*-alkanes and cycloalkanes. The highest yield of them, i.e., approximately 84 wt.%, was reached at 410 °C.

Some properties of the heaviest products, i.e., atmospheric residues, are shown in Table 5 to provide information about the hydrocracking products. From the point of view of raw material for hydrocracking, the products obtained from the mixed feedstock had a lower density and a slightly higher pour point. The dependence of sulfur and nitrogen content on the reaction temperature is the same as heavy naphtha and the middle distillate and is caused by the formation of aliphatic sulfur and nitrogen compounds during hydrocracking, especially at higher reaction temperatures. The distillation curves of the residues shifted to the lower boiling points with an increasing reaction temperature of the hydrocracking and with the presence of the PW in the feedstock.

Table 5. Physico-chemical properties of distillation residues obtained by hydrocracking of HVGO and HGVO containing 10 wt.% of petroleum wax (HVGO + PW) at various temperatures.

Parameter	390 °C		410 °C		430 °C	
	HVGO	HVGO + PW	HVGO	HVGO + PW	HVGO	HVGO + PW
Density at 15 °C ($kg \cdot m^{-3}$)	881.1	876.3	868.0	861.1	863.4	860.5
Sulfur ($mg \cdot kg^{-1}$)	1200	960	577	365	588	565
Nitrogen ($mg \cdot kg^{-1}$)	279	215	141	83	181	161
Pour point (°C)	36	39	33	36	33	36
Distillation [a]						
10 wt.% recovered at (°C)	396	390	388	380	384	379
50 wt.% recovered at (°C)	462	454	453	444	439	437
90 wt.% recovered at (°C)	532	517	523	518	500	512

[a] data obtained from simulated distillation.

3. Materials and Methods

3.1. Characteristics of the Feedstocks

Heavy vacuum gas oil (HVGO), obtained as a primary product of the oil vacuum distillation carried out at petroleum refinery ORLEN Unipetrol RPA (Litvínov, Czech Republic), was used as a basic feedstock for the hydrocracking. The HVGO was used as a feedstock for the reference experiments and as a major component for preparation of a mixed feedstock. The mixed feedstock was composed of 90 wt.% of the HVGO and 10 wt.% of the petroleum wax (PW), as obtained from the petroleum refinery dewaxing process. Its composition was determined using gas chromatograph equipped with mass spectrometer Focus (Thermo Electron Corporation, Waltham, MA, USA). Both components were blended at the temperature of 80 °C and homogenised. The components as well as the mixed feedstock were analysed by simulated distillation (SIMDIST). The analysis was carried out using a TRACE GC ULTRA (Thermo Fisher Scientific, Waltham, MA, USA) gas chromatograph equipped with an on-column injector, oven cryogenic cooling system and a capillary column Agilent (Santa Clara, CA, USA) J&W WCOT Ulti-metal (5 m × 0.53 mm i.d.: film thickness 0.17 μm). The refractive index of the HVGO, PW and the mixed feedstock was analysed using an Abbe-2WAJ Refractometer (PCE Instruments UK, Southampton, UK).

3.2. Hydrocracking

Hydrocracking of the feedstocks was performed in a bench-scale flow reactor equipped with a salt-bath heating system. The dimensions of the reactor were 614 mm (length) and 30 mm (inner diameter). A thermoprobe with an outer diameter of 9 mm was used, in which three thermocouples measuring temperature in the catalyst bed were located. The thermoprobe was placed in the centre of the reactor. The reactor was loaded with 90 g of the commercial amorphous-alumina-silica-supported Ni–W catalyst. A fresh catalyst was used for each type of feedstock. The catalyst was diluted in the volume of 1:1 with an inert, silicon carbide (size 0.1 mm) to ensure proper hydrodynamic conditions over the catalyst bed. SiC (size 1–2 mm) was placed in the reactor below and on the top of the catalyst bed. SiC in the lower part of the reactor (i.e., below the catalyst bed) ensured that the catalyst bed was located in the isothermal zone of the reactor. SiC in the upper preheating part of the reactor (i.e., above the catalyst bed) helped in the good mixing of the feedstock and hydrogen, before entering the catalyst bed. A standard catalyst-activation procedure using hydrogen sulfide was used. A certain amount of time was devoted to the stabilization of the catalyst activity. The temperature inside the reactor was monitored by means of three thermocouples. Adjustable positions of these thermocouples corresponded to the top, middle and bottom of the catalyst bed. A tempered feedstock container was placed on scales and thus the actual and average feed rates were recorded. The feedstock flow rate was kept at 72 $g \cdot h^{-1}$, which corresponds to a weight hourly space velocity (WHSV) of 0.8 h^{-1}. A constant hydrogen flow rate of 72 $Ndm^3 \cdot h^{-1}$ was controlled by a mass flow controller. The feedstocks (HVGO and the mixture of HVGO and 10 wt.% of petroleum wax) were hydrocracked at the reaction temperatures of 390, 410 and 430 °C under a hydrogen pressure of 18 MPa. The obtained primary liquid products were cooled down and collected in sealed vessels. In order to quickly assess the chemical composition changes, the refractive index of the primary products using an Abbe-2WAJ Refractometer (PCE Instruments UK, Southampton, UK) was determined.

3.3. Processing and Analysis of Products

A small part of all collected products was kept for the further analysis while the main portions were fractionated via distillation to obtain heavy naphtha (boiling range 100–200 °C), middle distillates (boiling range 200–360 °C) and residue (boiling range above 360 °C). A distillation apparatus (Fischer scientific, Waltham, MA, USA) with a SPALTROHR HMS 500 spiral column (Fischer scientific, Waltham, MA, USA) with 90 theoretical trays was used for the fractionation. The heavy naphtha fractions were obtained via atmo-

spheric distillation using the following parameters: reflux of 1:1, the maximum temperature in the distillation flask of 320 °C and the maximum temperature on the head of the distillation column of 200 °C. The middle distillates were obtained via vacuum distillation using the same reflux ratio, a pressure of 70 Pa, while the maximum temperature at the head of the column was 149 °C.

Three different gas chromatographic methods were used for the evaluation of the hydrocracking products. The SIMDIST method was always applied on all primary hydrocracking products and on all products obtained by their distillation.

The results of the SIMDIST analysis of the primary products were used for the calculation of the conversion (X_{360}) and the yield (Y_{360}) as follows:

$$X_{360} = 100 - Y_{360} \quad (1)$$

$$Y_{360} = Y_{LD/360} \times \frac{LR}{100} \quad (2)$$

where:

X_{360}: conversion to products having b. p. < 360 °C, wt. %.
Y_{360}: yield of residue (>360 °C), wt. % (based on feedstock)
$Y_{LD/360}$: yield of distillation residue (>360 °C) from SIMDIST, wt.%
LR: liquid products recovery from hydrocracking experiments, wt.% (b. p. > 100 °C, the samples do not include gases and light naphtha)

The heavy naphtha fractions and middle distillates were characterized in accordance with the ASTM D2887 method. The group-type analysis of naphtha samples was determined using an Agilent 6890 gas chromatograph (Agilent, Santa Clara, CA, USA) equipped with a split/splitless injector and a capillary column Agilent HP-PONA (50 m × 0.2 mm i.d.; film thickness 0.5 μm). All naphtha components were identified, quantified and assigned to the corresponding hydrocarbon group (*n*-alkanes, *iso*-alkanes, cycloalkanes, aromatics). The content of *n*-alkanes in the middle distillates was determined using a gas chromatograph Agilent 6890 (Agilent, Santa Clara, CA, USA) equipped with a split/splitless injector and a capillary column HP-ULTRA 1 (12 m × 0.32 mm i.d.; film thickness 0.52 μm). The content of *n*-alkanes was calculated as a sum of area percentage of all *n*-alkane peaks present in the chromatogram. The values obtained by this determination are not absolute, so they were used for comparison only. The determination of aromatic hydrocarbons in the middle distillates was performed using an HPLC system (Shimadzu, Kyoto, Japan) equipped with a refractometric detector and a Supelcosil column (St. Louis, MO, USA) LC-NH2-NP NP (25 cm × 4.6 mm i.d.; particle size 5 μm). This analysis was performed according to the EN 12916 standard test method.

The elemental composition of the selected samples and raw materials was determined using a Vario EL III (Elementar, Langenselbold, Germany) analyzer (determination of carbon and hydrogen) and TS-100/TN-100 (Mitsubishi, Tokyo, Japan) analyzer (determination of sulfur and nitrogen). The other properties, i.e., density (DMA 4000-Anton Paar, Graz, Austria), kinematic viscosity (SVM 3000-Anton Paar, Graz, Austria), water content (Coulometer WTK–Diram, Prague, Czech Republic), flash point (PMA 5-Anton Paar, Graz, Austria), cloud point and pour point (NTE 450–Normalab, Valliquerville, France) were determined using suitable standard test methods designated for petroleum products. The cetane index of middle distillates was calculated according to ISO 4264 method. Distillation data required for this calculation were obtained from API correlation proposed in the method ASTM D2887.

4. Conclusions

Hydrocracking of the neat heavy vacuum gas oil (HVGO) and its mixture with 10 wt.% petroleum wax at reaction temperatures 390; 410 and 430 °C and a pressure of 18 MPa was carried out. Although the addition of the petroleum wax (PW) to the feedstock led to mild conversion reduction, the quality of the primary liquid products obtained from

the blended feedstock was slightly better in most cases. The product obtained from the feedstock containing wax had a lower content of sulfur and nitrogen and lower density and refractive index. The moderate differences in group-type composition and in the density of heavy naphtha fractions obtained from the mixed feedstock were of negligible importance for their further processing. On the other hand, middle distillates prepared from the mixed feedstock had a slightly different group-type composition (differences did not exceed 20 relative percent) and a comparable or slightly lower density (differences did not exceed 5 $kg \cdot m^{-3}$). While the cloud point of all evaluated middle distillates was more or less identical (about -30 °C), middle distillates prepared from the mixed feedstock had a cetane index that was higher by up to 2 units as compared with those obtained from neat the HVGO. Middle distillates prepared from the feedstock containing petroleum wax, thus, can be described as a high-quality diesel component. Atmospheric residue obtained from the mixed feedstock can be used in the same way (base oil and heating oil production) as a similar distillation residue commonly prepared from the neat HVGO.

It can thus be concluded that products prepared by the hydrocracking of the feedstock containing petroleum wax had slightly better physicochemical properties than products from the neat HVGO hydrocracking. Due to the similarity in composition between the petroleum wax and Fischer-Tropsch wax it can be expected that the co-processing of FT wax as well as of petroleum waxes with a HVGO is feasible and would yield high-quality products.

Author Contributions: Data curation, O.P., A.V., D.M., M.Z. and P.S.; Formal analysis, O.P., A.V., M.Z. and P.S.; Funding acquisition, I.K.; Investigation, O.P. and D.M.; Methodology, D.S.; Project administration, O.P. and I.K.; Supervision, M.P.; Validation, O.P.; Visualization, O.P., A.V. and D.M.; Writing—review & editing, O.P., I.K., A.V., M.Z., D.S. and P.S. All authors have read and agreed to the published version of the manuscript.

Funding: This research received no external funding.

Acknowledgments: The work was supported by the Ministry of Education, Youth and Sports of the Czech Republic from the institutional support of the research organisation (CZ60461373). The result was achieved using the infrastructure included in the project Efficient Use of Energy Resources Using Catalytic Processes (LM2018119) which has been financially supported by MEYS within the targeted support of large infrastructures.

Conflicts of Interest: The authors declare no conflict of interest.

References

1. Edenhofer, O.; Pichs-Madruga, R.; Sokona, Y.; Seyboth, K.; Kadner, S.; Zwickel, T.; Eickemeier, P.; Hansen, G.; Schlömer, S.; von Stechow, C. *Renewable Energy Sources and Climate Change Mitigation: Special Report of the Intergovernmental Panel on Climate Change*; Cambridge University Press: Cambridge, UK, 2011.
2. Qazi, A.; Hussain, F.; Rahim, N.A.; Hardaker, G.; Alghazzawi, D.; Shaban, K.; Haruna, K. Towards sustainable energy: A systematic review of renewable energy sources, technologies, and public opinions. *IEEE Access* **2019**, *7*, 63837–63851. [CrossRef]
3. Mathew, G.M.; Raina, D.; Narisetty, V.; Kumar, V.; Saran, S.; Pugazhendi, A.; Sindhu, R.; Pandey, A.; Binod, P. Recent advances in biodiesel production: Challenges and solutions. *Sci. Total Environ.* **2021**, *794*, 148751. [CrossRef] [PubMed]
4. Kubičková, I.; Kubička, D. Utilization of triglycerides and related feedstocks for production of clean hydrocarbon fuels and petrochemicals: A review. *Waste Biomass Valorization* **2010**, *1*, 293–308. [CrossRef]
5. Tomasek, S.; Lonyi, F.; Valyon, J.; Wollmann, A.; Hancsók, J. Hydrocracking of Fischer–Tropsch Paraffin Mixtures over Strong Acid Bifunctional Catalysts to Engine Fuels. *ACS Omega* **2020**, *5*, 26413–26420. [CrossRef]
6. Rao, T.M.; Dupain, X.; Makkee, M. Fluid catalytic cracking: Processing opportunities for Fischer–Tropsch waxes and vegetable oils to produce transportation fuels and light olefins. *Microporous Mesoporous Mater.* **2012**, *164*, 148–163.
7. Robinson, P.R.; Dolbear, G.E. Hydrotreating and hydrocracking: Fundamentals. In *Practical Advances in Petroleum Processing*; Springer: Berlin/Heidelberg, Germany, 2006; pp. 177–218.
8. Prado, C.M.; Antoniosi Filho, N.R. Production and characterization of the biofuels obtained by thermal cracking and thermal catalytic cracking of vegetable oils. *J. Anal. Appl. Pyrolysis* **2009**, *86*, 338–347. [CrossRef]
9. Dik, P.; Danilova, I.; Golubev, I.; Kazakov, M.; Nadeina, K.; Budukva, S.; Pereyma, V.Y.; Klimov, O.; Prosvirin, I.; Gerasimov, E.Y. Hydrocracking of vacuum gas oil over NiMo/zeolite-Al_2O_3: Influence of zeolite properties. *Fuel* **2019**, *237*, 178–190. [CrossRef]
10. Klerk, A.D. Fischer–Tropsch fuels refinery design. *Energy Environ. Sci.* **2011**, *4*, 1177–1205. [CrossRef]

11. Kubička, D. Future refining catalysis-introduction of biomass feedstocks. *Collect. Czechoslov. Chem. Commun.* **2008**, *73*, 1015–1044. [CrossRef]
12. Leckel, D. Hydrocracking of iron-catalyzed Fischer–Tropsch waxes. *Energy Fuels* **2005**, *19*, 1795–1803. [CrossRef]
13. De Klerk, A. Thermal cracking of Fischer–Tropsch waxes. *Ind. Eng. Chem. Res.* **2007**, *46*, 5516–5521. [CrossRef]
14. Fernandes, F.A.; Teles, U.M. Modeling and optimization of Fischer–Tropsch products hydrocracking. *Fuel Process. Technol.* **2007**, *88*, 207–214. [CrossRef]
15. Dupain, X.; Krul, R.A.; Schaverien, C.J.; Makkee, M.; Moulijn, J.A. Production of clean transportation fuels and lower olefins from Fischer-Tropsch Synthesis waxes under fluid catalytic cracking conditions: The potential of highly paraffinic feedstocks for FCC. *Appl. Catal. B Environ.* **2006**, *63*, 277–295. [CrossRef]
16. Lappas, A.A.; Iatridis, D.K.; Vasalos, I.A. Production of liquid biofuels in a fluid catalytic cracking pilot-plant unit using waxes produced from a biomass-to-liquid (BTL) process. *Ind. Eng. Chem. Res.* **2011**, *50*, 531–538. [CrossRef]
17. Kubicka, D.; Černý, R. Upgrading of Fischer–Tropsch waxes by fluid catalytic cracking. *Ind. Eng. Chem. Res.* **2012**, *51*, 8849–8857. [CrossRef]
18. Šimáček, P.; Kubička, D.; Pospíšil, M.; Rubáš, V.; Hora, L.; Šebor, G. Fischer–Tropsch product as a co-feed for refinery hydrocracking unit. *Fuel* **2013**, *105*, 432–439. [CrossRef]
19. Palou, A.; Cruz, J.; Blanco, M.; Larraz, R.; Frontela, J.; Bengoechea, C.S.M.; González, J.M.; Alcalà, M. Characterization of the composition of petroleum waxes on industrial applications. *Energy Fuels* **2014**, *28*, 956–963. [CrossRef]
20. Pfennig, A. Kirk-Othmer Encyclopedia of Chemical Technology, 4th Ed., Vol. 10. M. Howe-Grant (Editor). John Wiley & Sons, New York 1993. 1022 S. mit zahlr. Abb. und Tab., geb., £ 185.00. *Chem. Ing. Tech.* **1995**, *67*, 352–353. [CrossRef]
21. Goetzmann, S.; Kreuter, W.; Wernicke, H. Hydroconversion upgrades heavy olefin feedstocks. *Hydrocarb. Process (US)* **1979**, *58*, 6.
22. Ward, J.W. Hydrocracking processes and catalysts. *Fuel Process. Technol.* **1993**, *35*, 55–85. [CrossRef]
23. Nowak, S.; Zimmermann, G.; Guschel, H.; Anders, K. New routes to low olefins from heavy crude oil fractions. In *Studies in Surface Science and Catalysis*; Elsevier: Amsterdam, The Netherlands, 1989; Volume 53, pp. 103–127.
24. Hoehn, R.; Thakkar, V.; Yuh, E. *Hydroprocessing for Clean Energy: Design, Operation, and Optimization*; John Wiley & Sons: Hoboken, NJ, USA, 2017.
25. Thybaut, J.W.; Laxmi Narasimhan, C.; Denayer, J.F.; Baron, G.V.; Jacobs, P.A.; Martens, J.A.; Marin, G.B. Acid–metal balance of a hydrocracking catalyst: Ideal versus nonideal behavior. *Ind. Eng. Chem. Res.* **2005**, *44*, 5159–5169. [CrossRef]
26. Leckel, D.; Liwanga-Ehumbu, M. Diesel-selective hydrocracking of an iron-based Fischer–Tropsch wax fraction (C15–C45) using a MoO_3-modified noble metal catalyst. *Energy Fuels* **2006**, *20*, 2330–2336. [CrossRef]
27. Leckel, D. Noble metal wax hydrocracking catalysts supported on high-siliceous alumina. *Ind. Eng. Chem. Res.* **2007**, *46*, 3505–3512. [CrossRef]
28. Halmenschlager, C.M.; Brar, M.; Apan, I.T.; de Klerk, A. Hydrocracking vacuum gas oil with wax. *Catal. Today* **2020**, *353*, 187–196. [CrossRef]
29. Baragi, J.G.; Maganur, S.; Malode, V.; Baragi, S.J. Excess molar volumes and refractive indices of binary liquid mixtures of acetyl acetone with n-Nonane, n-Decane and n-Dodecane at (298.15, 303.15, and 308.15) K. *J. Mol. Liq.* **2013**, *178*, 175–177. [CrossRef]
30. Kallo, D.; Onyestyak, G.; Papp, J., Jr. An IR study of the surface species present on zeolite catalysts in some simple addition reactions. *J. Mol. Catal.* **1989**, *51*, 329–340. [CrossRef]
31. Deeba, M.; Ford, M.E.; Johnson, T.A. Direct amination of ethylene by zeolite catalysis. *J. Chem. Soc. Chem. Commun.* **1987**, 562–563. [CrossRef]
32. Calemma, V.; Ferrari, M.; Rabl, S.; Weitkamp, J. Selective ring opening of naphthenes: From mechanistic studies with a model feed to the upgrading of a hydrotreated light cycle oil. *Fuel* **2013**, *111*, 763–770. [CrossRef]